Korea-Australia Rheology Journal
Vol. 19, No. 3, November 2007 pp. 157-164

Spherical and cylindrical microencapsulation of living cells using microfluidic devices

Joung Sook Hong[1,2], Su Jung Shin[1], SangHoon Lee[1], Edeline Wong[3] and Justin Cooper-White[3]*
[1]*Department of Biomedical Engineering, Korea University, Anam-dong, Sungbuk-ku, Seoul 136-703, Korea*
[2]*Department of Chemical and Biological Engineering, Korea University, Anam-dong, Sungbuk-ku, Seoul 136-713, Korea*
[3]*Australian Institute for Bioengineering and Nanotechnology, The University of Queensland, St. Lucia, Qld 4072, Australia*
(Received July 4, 2007; final revision received October 12, 2007)

Abstract

Microencapsulation of cells within microfluidic devices enables explicit control of the membrane thickness or cell density, resulting in improved viability of the transplanted cells within an aggressive immune system. In this study, living cells (3T3 and L929 fibroblast cells) are encapsulated within a semi-permeable membrane (calcium crosslinked alginate gel) in two different device designs, a flow focusing and a core-annular flow focusing geometry. These two device designs produce a bead and a long microfibre, respectively. For the alginate bead, an alginate aqueous solution incorporating cells flows through a flow focusing channel and an alginate droplet is formed from the balance of interfacial forces and viscous drag forces resulting from the continuous (oil) phase flowing past the alginate solution. It immediately reacts with an adjacent $CaCl_2$ drop that is extruded into the main flow channel by another flow focusing channel downstream of the site of alginate drop creation. Depending on the flow conditions, monodisperse microbeads of sizes ranging from 50-200 μm can be produced. In the case of the microfibre, the alginate solution with cells is extruded into a continuous phase of $CaCl_2$ solution. The diameter of alginate fibres produced via this technique can be tightly controlled by changing both flow rates. Cell viability in both forms of alginate encapsulant was confirmed by a LIVE/DEAD cell assay for periods of up to 24 hours post encapsulation.

Keywords : calcium alginate gel, bead, fibre, microencapsulation, microfluidics

1. Introduction

Immune protection of cells using encapsulation technology has been proposed as a notable method to improve cellular viability following transplantation (Chang, 1964). Cells are surrounded by a semi-permeable biocompatible membrane, which allows low molecular weight nutrients and metabolites, including hormones, to pass through to the encapsulated cells, but excludes larger antibodies and cytotoxic cells of the host, thus immuno-protecting the implant. This technology has been applied in the transplantation of pancreatic islet cells into diabetic animals (Lim and Sun, 1980; Sun *et al.*, 1996), for the treatment of hormone or protein deficient diseases, and for cancer therapy. However, there are still several problems to be solved. The first is to find biocompatible polymers for the semi-permeable membrane which satisfy various desires such as biocompatibility and immunoisolation (Lacy and Kostianovsky 1967; Fan *et al.*, 1990; Khattak *et al.*, 2005). The other is an improved methodology to encapsulate a desired number of cells within a desired geometry. Attempts to resolve some of these limitations in encapsulation has led the development of microencapsulation technology, making it possible to control size explicitly per drop, rather than bulk emulsification methods often employed.

The use of microencapsulation technology to generate smaller beads has many advantages with regards to improved nutrient and oxygen transfer to cells, and enhanced mechanical strength, both of which result in better in vivo efficacy. Polyelectrolyte biopolymers have often been used as base gel component materials in microbead encapsulation, due to the relative ease with which these systems gel simply by the presence of divalent ions (Fan *et al.*, 1990; Lim and Sun, 1980; Sun *et al.*, 1996). For example, as soon as an aqueous alginate solution is contacted with Ca^{2+} ions, the solution is immediately transformed into a gel by ionic crosslinking at the guluronic acid sites on adjacent alginate chains. To complete gelation, it takes from a few seconds to a few minutes depending on the diffusion of Ca^{2+} ions in the solution, which in turn is dependent on the concentration of calcium. Unfortunately, an ionic-crosslinked alginate gel is easily degraded when put into a solution which is lower in or absent of calcium. To avoid such a problem, these gels can be crosslinked using a macromolecular polycation, such as poly-L-lysine, which sus-

*Corresponding author: j.cooperwhite@uq.edu.au

tains the structure for longer time period (Strand, 2001), or covalently crosslinked to improve the term mechanical stability using, for example, a photo-active cross-linker. The vibrating nozzle or coaxial air-flow methods are widely used techniques in encapsulation fields, resulting in beads of sizes ranging from 160-800 μm (Sugiura *et al.*, 2005). Microencapsulation methods can however generate beads or capsules of smaller sizes and more uniform distributions (Utada *et al.*, 2005). However, although successful at encapsulating a given payload (i.e. cells), further detailed understanding of the mechanism of encapsulation is required to invoke the desired control over bead size or local (bead) cell density.

In this study, we have encapsulated two cell lines (fibroblasts 3T3 and L929) through the use of two different microfluidic geometries, planar co-flow and core-annular flow. The microfluidic channel based on planar flow controls the width of the central stream through the application of hydrodynamic stress by two side streams, which is used in this work to generate cell-loaded gel microparticles. In order to produce a fibre loaded with the requisite cells, a continuous generation method based on core-annular flow, coined the '*on the fly*' process (Jeong *et al.*, 2004 and 2005), was used. This process has many practical advantages in the production of micro-fibres, such as easy control of size and controlled loading of biological materials. The dependence of the resulting size of the bead or fibre produced on the flowrate of each phase and the alginate concentration was examined. After encapsulation, we confirmed the viability of the cells using the LIVE/DEAD assay.

2. Experiments

2.1. Materials

Sodium alginate powder was purchased from Sigma-Aldrich Chem. Co. and a 1wt% alginate solution was prepared by gentle roll mixing for 1 day. Calcium chloride powder from Sigma Chem. Co. was used to prepare 0.13M $CaCl_2$ solutions. Oil (sunflower oil) was used as the continuous phase to generate alginate droplets.

2.2. Rheological measurement

The rheological properties of the aqueous alginate solutions and alginate gels were measured using a stress-controlled rheometer (G2 from TA instruments) with a parallel plate fixture (diameter 20 mm). The gap between the two plates was set at 0.9-1.2 mm to prevent wall effects during measurement. For steady shear viscosity, steady stress sweep tests were conducted over the stress range from 0.01 Pa to 100 Pa.

2.3. Fabrication of microfluidic devices

Fig. 1 and Fig. 2 show schematic diagrams of the microfluidic devices used in this study. Fig. 1 is for bead formation and Fig. 2 is for microfibre formation. The flow-focusing channel (A of Fig. 1(a)) was fabricated based on standard photolithographic procedures with polydimethylsiloxane (PDMS) and a SU-8 photoresist mold using soft-lithography (Li, 2006). The flow focusing channel is presented in detail in Fig. 1(b). The microfluidic device used for fibre generation (see Fig. 2(a)) was fabricated by combining the PDMS platform and a 'pulled' borosilicate glass pipette, as seen in detail in Fig. 2(b) (Jeong *et al.* 2004 and 2005). A 3-D bi-coaxial stream of the continuous phase flows around the core flow of the dispersed phase (alginate solution) at the point where the two flows merged. Once both fluids have contacted each other, the alginate gel is spontaneously produced at the interface by the rapid ionically-induced cross-linking reaction. Downstream, the

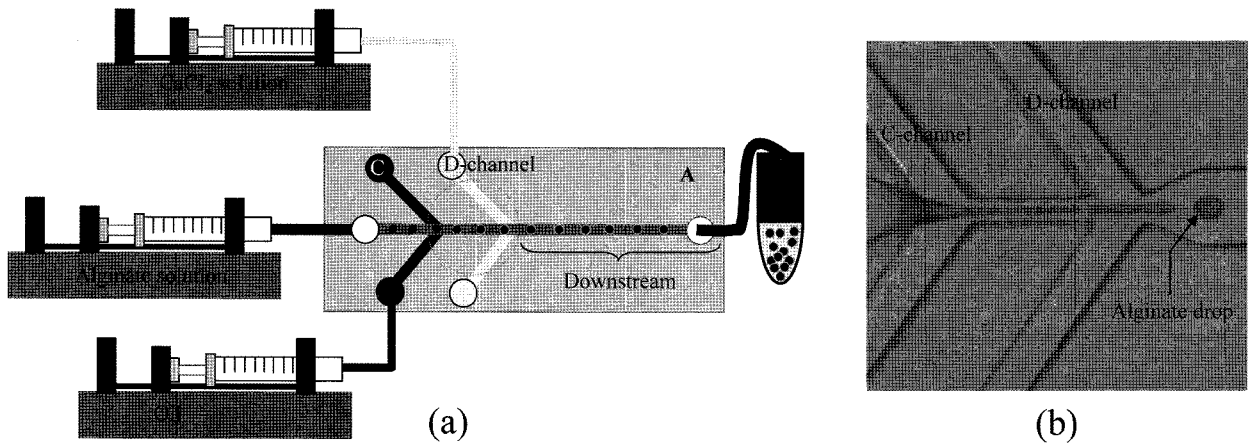

Fig. 1. (a) Schematic diagram of the microfluidic process for calcium alginate bead formation and (b) a top view of the flow focusing channel in detail (the dotted circle in Fig. 1(a)). The width of the core, flow focusing (C- and D- channel), and downstream channels are 40 μm, 100 μm, and 200 μm respectively, while the length of the downstream section is 1cm, and the overall thickness is 200 μm.

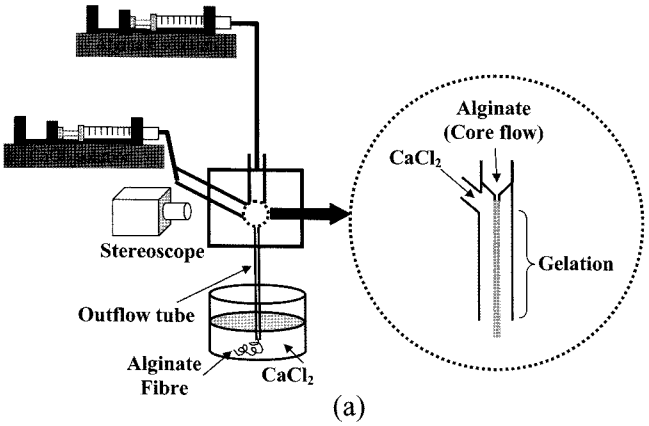

(a)

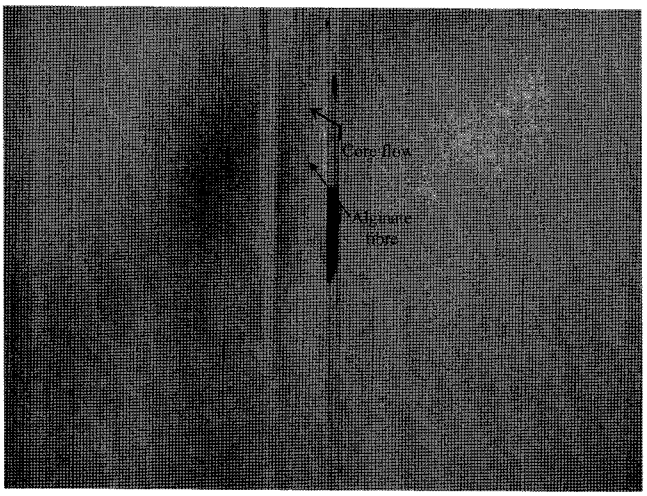

(b)

Fig. 2. (a) Schematic diagram of the microfluidic process for calcium alginate microfibre formation and (b) a side view of the core-annular flow focusing channel in detail. The diameter of the core channel and the annular flow focusing channel are 30 μm and 750 μm, while the length of downstream section is 3 cm.

gelation of the cylindrical fibres was further matured by diffusion of the cation (Ca^{2+}) throughout the alginate system. We extended the reaction time between sodium alginate and Ca^{2+} ions to complete the gelation by simply employing a longer downstream channel.

2.4. Cell-preparation

To demonstrate the applicability of alginate fibres or beads as cell carriers for drug delivery and tissue engineering applications, we encapsulated fibroblast cells (L929 and 3T3). Fibroblast cells were initially expanded in 6 well plates within Dulbecco's Modified Eagle Medium (DMEM, GIBCO) with 10% Fetal Bovine Serum (FBS, GIBCO) and 1% antibiotics containing 10,000 units (GIBCO) of penicillin and streptomycin, at 37°C under 5% CO_2. Cells were detached from the wells for use within the microdevices with a solution of 0.25% trypsin/EDTA (GIBCO) for 2-3 minutes at 37°C.

3. Results

The gelation time for these hydrogels, mediated by the cross-linking of alginate chains with Ca^{2+} ions, is governed principally by the available concentration of Ca^{2+} ions and the diffusion coefficient of calcium in the alginate solution. Increases in either the calcium concentration or alginate concentration will significantly effect the time required to form gels of appropriate character. It is therefore paramount that the local concentration of $CaCl_2$ and the appropriate residence times for the maturation of a gelled network are controlled. Microfluidic devices offer significant advantages in this extent, in that the flow is laminar and hence the diffusive transport of ions is predictable and is the dominant mode of mass transfer. In addition, time for maturation of structure can be changed simply by changing the length of the channel post formation of the drop or fibre.

The reaction between alginate and Ca^{2+} is very rapid, that is, a few seconds. Due to this very rapid timeframe, it was impossible to follow the gelation of the alginate:calcium system within the rheometer. In any case, within the microdevices, the alginate is not directly exposed to calcium until after the formation of the drop, and hence the changes in viscosity of the system during calcium ingress are irrelevant to the drop formation event. The viscosities of the alginate solution and the sunflower oil are matched (see Fig. 3), meaning that the effect of viscosity on drop formation is minimal and the resulting drop size is principally the result of a force balance between drag forces applied by the sunflower oil and the interfacial tension forces holding the dispersed phase (alginate solution) to the nozzle within each of the devices.

The relationship between drop size and fluid properties for these geometries is not the subject of this paper and is described in detail in Hong and Cooper-White (2007). Instead, we focus in this study on the final properties of the gel with respect to their response to steady shear, as it is the value of the yield stress that is important in terms of the robustness of these capsules within in vitro culture and in vivo utilization. When an alginate solution is added to a $CaCl_2$ solution, the system viscosity increases by over 5 orders of magnitude, regardless of the concentration of alginate varying from 0.5-1.0%, as seen in Fig. 3. As also shown in Fig. 3, the shear viscosity of the resultant alginate gel also varies depending on the volume ratios of alginate: Ca^{2+}. Above a certain shear rate or stress, these gels yield and fracture (irreversibly). For the 0.5% alginate, the yield stress is approximately 10Pa, while for 1% alginate, it is between 30-70 Pa. These values of yield stress are relatively low and the rupture resilience of microparticles and

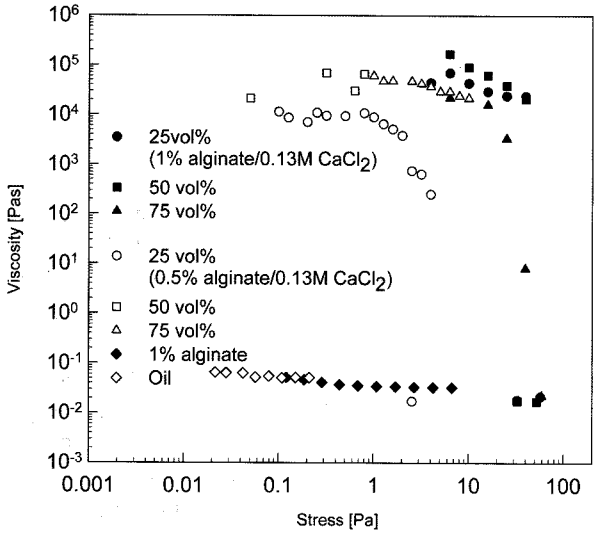

Fig. 3. Rheological behaviour of 0.5 and 1% alginate solution, sunflower oil and alginate gels of different volume ratios of alginate: 0.13 M $CaCl_2$ solution.

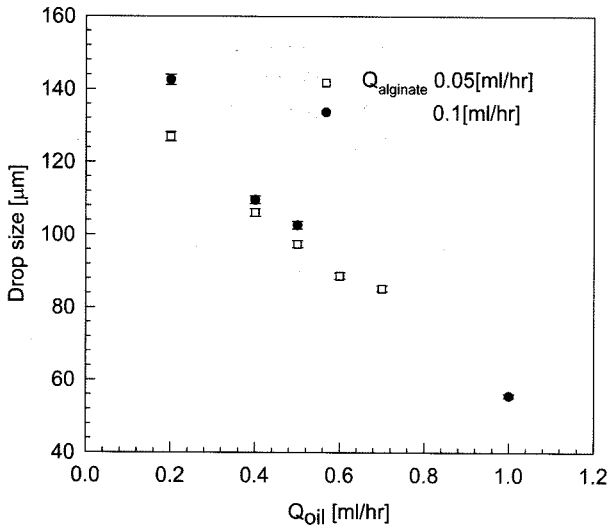

Fig. 4. Variation of drop size with continuous phase (sunflower oil) flow rate. The flow rate of the alginate solution was fixed at 0.1 or 0.05 ml/hr, and that of $CaCl_2$ solution was fixed to 0.05 ml/hr.

microfibres when delivered through a needle is currently being investigated. However, the stresses seen by the particles within the microdevices are below these values (there is no contact with the walls of the device) and no stress-induced breakup of the particles post manufacture was observed within the devices.

3.1. Formation of microbeads

Fig. 1 presents the schematic diagram of the microfluidic device used to generate the gelled microbeads. Through the central channel, an aqueous sodium alginate solution is extruded into oil. The oil flows through the C-channel and

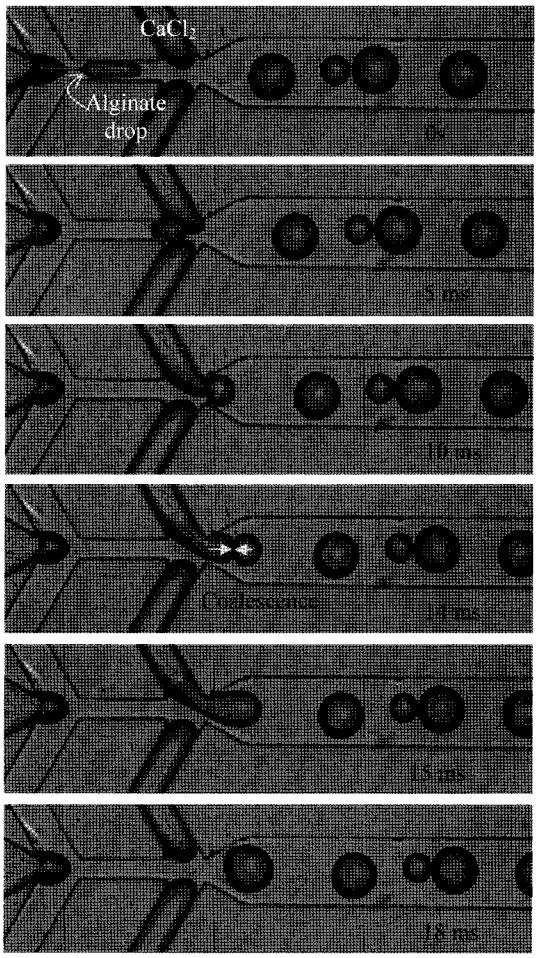

Fig. 5. Coalescence of the alginate drop with the $CaCl_2$ drop (a) after flow focusing and (b) movement of the gelling drop downstream. The flow condition is 0.1 ml/hr for alginate, 0.4 ml/hr for sunflower oil, and 0.05 ml/hr for the $CaCl_2$ solution.

the $CaCl_2$ solution flowing through D-channel focuses the central stream at the flow focusing point. A flow focusing geometry is one of the most prevalent designs to generate a monodisperse drop (Anna *et al.*, 2003). It has been utilized by Xu and Nakajima (2004), for example, to control the drop size by hydrodynamically focusing the narrow central stream to a critical width and the breakup of central stream then is the result of a Rayleigh instability (1879). The oil flowing through the C-channel controls the width of alginate stream through the central channel and the pinching off of the drop.

The dependence of the drop size on the flow rate of the continuous phase was investigated. The flow rate of oil was varied from 0.1 to 10.0 ml/hr. In general, as seen in Fig. 4, the drop size of the alginate solution is decreased as the flow rate of oil increases. As expected, at the same oil flow rate, as the flow rate of the alginate solution was increased, the drop size was increased. The addition of cells to the alginate solution does not change the drop size.

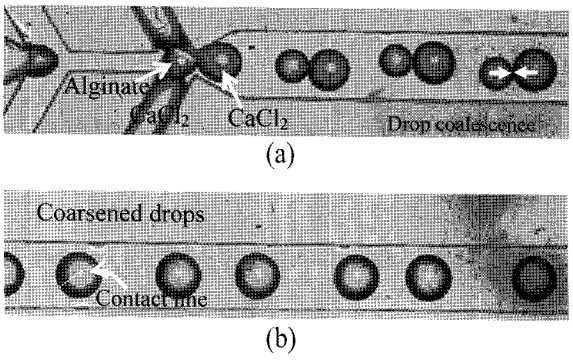

Fig. 6. Alginate drop formation and its coalescence with a $CaCl_2$ drop at the flow focusing junction. The flow condition is 0.1 ml/hr for alginate, 0.5 ml/hr for sunflower oil, and 0.05 ml/hr for the $CaCl_2$ solution.

Successful coalescence of the alginate: calcium solution was observed to be very dependent on the flow rate of the oil phase, the alginate solution and the $CaCl_2$ solution. There were two ways to combine the alginate drop and $CaCl_2$ drop-coalescence at the second flow-focusing point (Fig. 5) or coalescence during downstream flow (Fig. 6). Fig. 5 exemplifies the coalescence event between the alginate drop and $CaCl_2$ stream at the second flow focusing point. At the flow focusing point, the $CaCl_2$ stream restricts the forward motion of the alginate drop, encouraging early contact and optimal 'programmed' coalescence. There is thereafter effective mixing between the two phases during coalescence. If, on the other hand, the two drops coalesce further downstream, as seen in Fig. 6, homogeneous gelation inside the combined drop is inhibited. When the two drops are combined, a contact line between the two fluids is preserved for some time (see Fig. 6(b)) prior to the formation of a gelled particle further downstream. In order to improve the mixing between the alginate and Ca^{2+} ions, the coalesced drop requires a longer path length (traveling time) or an effective geometrical change (for example, a contraction). At oil flowrates of between 0.4 and 0.5 ml/hr, the alginate drops are consistently coalesced with $CaCl_2$ drops, as seen in both Fig. 5 and Fig. 6.

Based on the outcomes of this investigation, alginate solutions incorporating live fibroblast cells were used to generate microbeads at the following flowing flow conditions: 0.1 ml/hr for alginate solution with cells, 0.5 ml/hr for sunflower oil, and 0.05 ml/hr for the $CaCl_2$ solution. This particular combination was chosen as it resulted in consistent mixing of the two dispersed phases at the second flow focusing point and hence consistent formation of monodisperse cell-loaded alginate microbeads. The cells plus media, post trypsinisation from the culture well plates, were first centrifuged and a concentrated cell suspension (of 10^5 cells/ml) was added to a small amount of calcium-deficient phosphate buffered saline (PBS, Invitrogen). The rheological behaviour of the calcium alginate gel was not

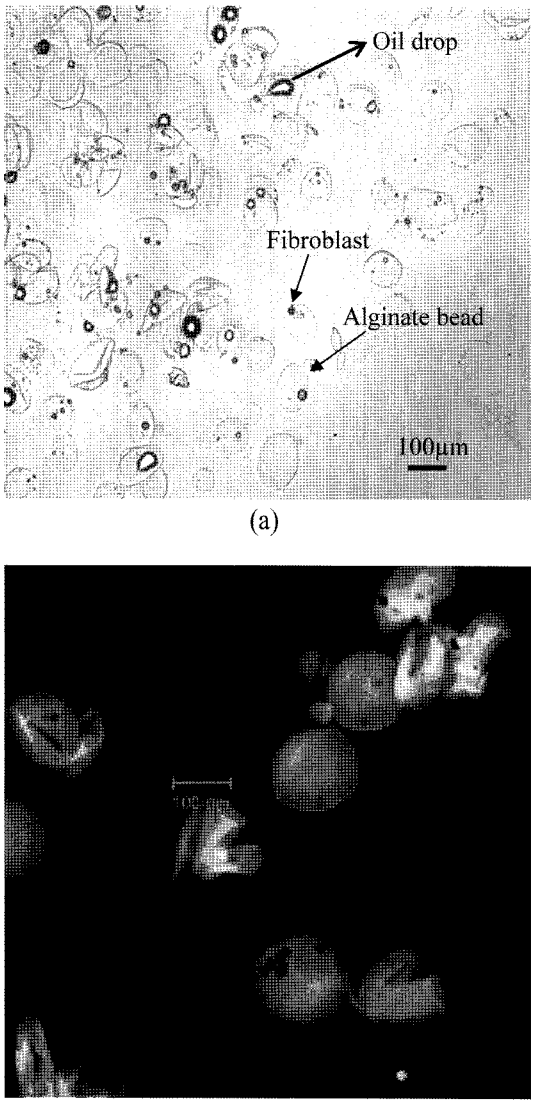

Fig. 7. Images of alginate beads containing cells after collection at the outflow of the device. Flow conditions were 0.05 ml/hr for alginate, 0.5 ml/hr for oil, and 0.05 ml/hr for the $CaCl_2$ solution. (a) Image from optical microscope and (b) from florescence microscope.

changed by the addition of PBS (up to 20 vol% for 1% alginate solution, data not shown). 1 ml of the cell suspension was added to 4 ml of alginate solution and it was then introduced into the central channel of the microdevice, as per previous experiments. The cell encapsulated alginate beads were collected at the outflow of the channel, as shown in Fig. 1(a), and they were then introduced into a $CaCl_2$ solution (0.13 M) to separate beads from the oil and to allow further maturation of the gelled particles.

Fig. 7 presents a picture of cells encapsulated within the alginate beads. The bead size was noted to vary between 120 and 200 μm. It is likely that some of beads were destroyed during transfer from the device to the $CaCl_2$ solu-

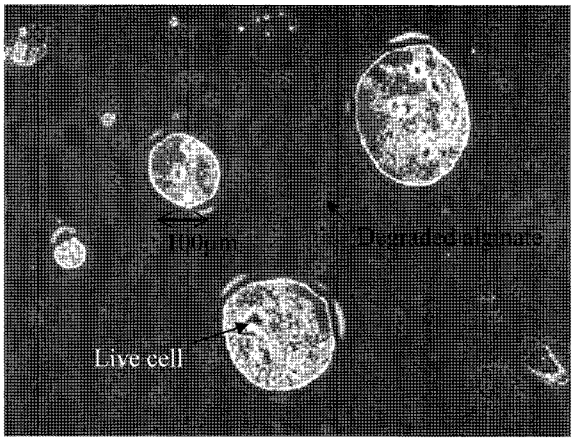

Fig. 8. LIVE/DEAD Assay of cells encapsulated within the alginate bead. Each bead includes one to six cells. During the LIVE/DEAD assay, some alginate gel particles were seen to degrade due to the change in the buffer conditions (lower calcium concentrations than within the beads resulted in elution of calcium and breakdown of the beads).

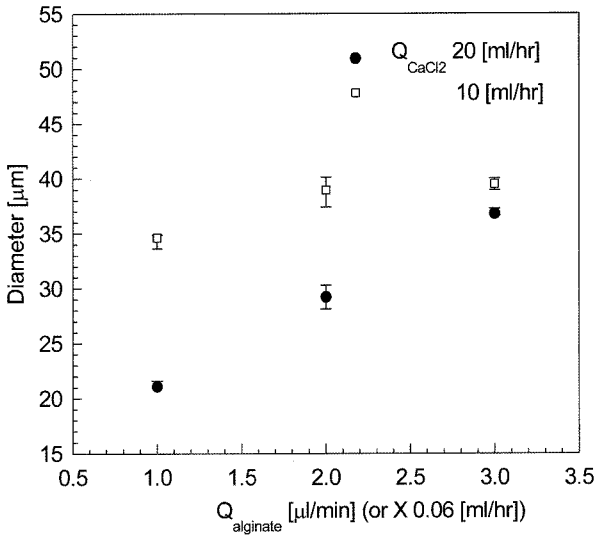

Fig. 9. Variation in the diameter of microfibre depending on core flow rate, 1.0 to 3.0 μl/min. The flow rate of the $CaCl_2$ solution is fixed to 10 or 20 ml/hr.

tion as a result of the alginate gel not being homogeneously gelled throughout, a result of a heterogeneous distribution of Ca^{2+} ion inside alginate bead in the absence of good mixing between the alginate-cell suspension and the calcium chloride solution. The separation procedure was not 100% effective, as we still observed a few oil drops within the alginate bead suspension. Explicit control over the number of cells within each bead was not attempted but it is obvious that this can be afforded by simply changing the concentration of cells added to the alginate solution prior to droplet formation.

To check the cells were viable post encapsulation, we utilized a LIVE/DEAD assay. LIVE/DEAD assay reagents (LIVE/DEAD® Viability/Cytotoxicity#1 (L-7013)) were dissolved following the procedure defined by Microprobes (Product information MP07013). The cell-loaded beads were not transferred to normal cell culture media, but left within the 0.13 M calcium alginate solution for a period of 5 hours. The labeled cells were then observed using a fluorescence microscope, with live cells being green and dead cells being red. Fig. 8 shows that most of the cells inside the beads were alive post 5hrs after encapsulation.

3.2. Formation of microfibres

Fig. 2 is a schematic of the microfibre generation device. Alginate solution flows directly into the 0.13 M $CaCl_2$ solution through the core channel. The solution properties (namely the high viscosity of the alginate phase and the very low interfacial tension between the disperse and continuous phases) and the geometry favour the formation of a microfibre rather than a drop, as shown in Fig. 2(a). Fig. 2(b) presents the generation of a 'curled' fibre near the coaxial point. To enhance the contrast between these two phases, a small amount of Papicel Red IJ-F3B (Eastwell) was added to the alginate solution. The morphology of the alginate stream obviously varied considerably depending on the ratio of the disperse : continuous phase flow rates. At low ratios (less than 0.003), straight fibres of the alginate are produced, representing a predominantly laminar flow field of both phases, and fibre diameters can be explicitly controlled through variations in the flowrates of either alginate or calcium choride solutions (Figure 9). At ratios above 0.015, a 'curled' core fluid stream was produced. For example, as the core flow rate was increased from 1 to 5 μl/min at a fixed annular flow of 20 ml/hr, the alginate stream curled as shown in Fig. 2(b). As the core flow rate was further increased, the 'curl' frequency increased. The curvature noted in the fibres during formation is likely to be a result of gelation of the alginate which now occurs at the contract line between the alginate and calcium solution as soon as it exits the nozzle surface. This gel transition will rapidly increase the viscosity and also produce surface contracture as a result of densification of the alginate phase. The flow downstream of the nozzle will also be significantly perturbed by the rapid introduction of the forming alginate fibre, introducing flow instabilities not seen at lower core flow rates. Unfortunately, once an alginate fibre forms spiral curls, such an alginate sample flow causes clogging of the outflow. In addition, as the flow rate increases, the residence time of fibre is not enough to ensure complete gelation.

In cell-loading experiments, the flow conditions were fixed at 1 μl/min for the alginate solution and 20 ml/hr for the $CaCl_2$ solution. Additionally, the outflow tube was extended up to 3 cm to allow gelation of the formed fibres.

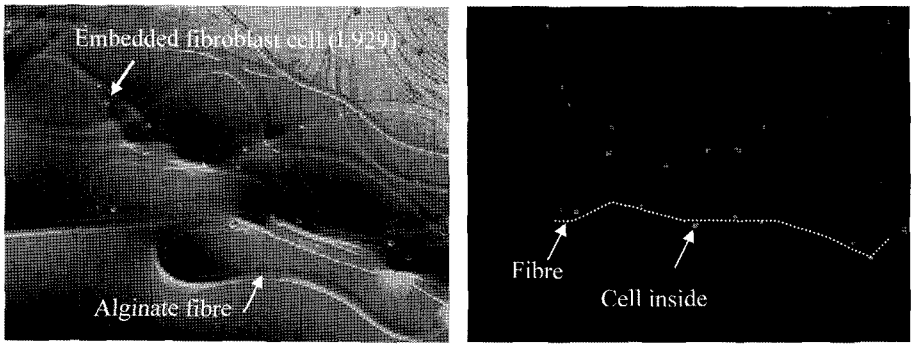

(a) (b)

Fig. 10. Images of cells embedded within the alginate fibre after cell encapsulation (1 hr). Flow condition is 1.0 μl/min for alginate and 20.0 ml/hr for the $CaCl_2$ solution. (a) Image from optical microscope (the average width of microfibre is ~20 μm) and (b) from florescence microscope. Cells embedded in the alginate fibre are stained with cell tracker (Red CMTPX, Invitrogen).

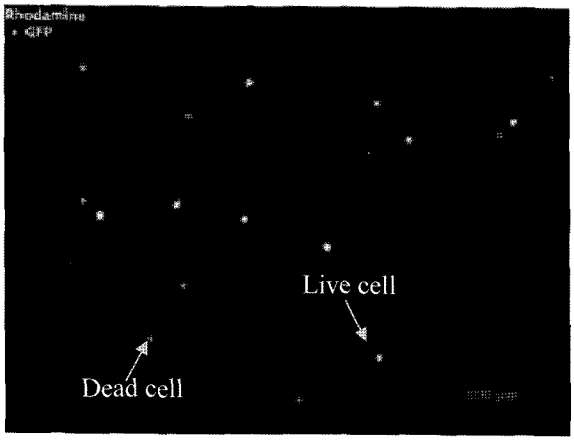

Fig. 11. LIVE/DEAD Assay of cells embedded in the alginate fibre after 24 hrs following encapsulation. Green denotes live cells and red, dead cells.

Using these conditions, the cells were sequentially loaded along the flow direction of the fibre, as shown in Fig. 10. The local density of cells within the fibre could be controlled by increasing the initial seeding density within the alginate solution or by changing the diameter of core flow (in Fig. 10, ~30 μm).

The viability of the cells within the fibres was checked using the LIVE/DEAD assay immediately after encapsulation and after 24 hours. For the 24 hour timepoint, the cell embedded fibres were incubated in the same culture media and culture conditions as previously described. These experiments confirmed the viability of these cells within the microfibres for this period of time (see Fig. 11). Longer timepoints investigating the capability for cell expansion and microfibre stability are underway.

4. Conclusions

This study reports the generation of calcium crosslinked alginate beads or microfibres and the on-line encapsulation of living cells using two microfluidic methods, flow focusing and core-annular flow focusing. The mechanism of encapsulation was investigated with respect to alginate : calcium ratios and changes in flow rate of continuous and dispersed phases. The size of the monodisperse alginate beads can be explicitly controlled to within a range of 50-200 μm, depending on flow condition, with similar control being invoked over the diameter of alginate microfibres. This control over bead or fibre lengthscales affords therefore control over the thickness of the alginate gel membrane surrounding the cells, preventing any barriers to oxygen or nutrient transport for optimum cell viability. Using these microfluidic devices, fibroblast cells (NIH 3T3 and L929) were successfully encapsulated within the calcium alginate gels, with the local cell density within the beads or fibres being controlled through changes in the flowrates of dispersed and continuous phases and the initial concentration of cells introduced into the alginate solution prior to bead or fibre formation. Cell viability was confirmed using the LIVE/DEAD cell assay for a period of up to 24 hours. These microdevice designs show significant potential in their provision of bead or fibre-based systems for in vivo cell-based drug delivery and tissue engineering applications.

References

Anna, S.L., N. Bontoux and H.A. Stone, 2003, Formation of dispersions using "flow focusing" in microchannels, *App. Phy. Lett.* **82(3)**, 364-366.

Chang, T.M.S., 1964, Semipermeable microcapsule, *Science* **146**, 524-525.

Fan, M.Y., Z.P. Lum, X.W. Fu, L. Levesque, I.T. Tai and A.M. Sun, 1990, Reversal of diabetes in BB rats by transplantation of encapsulated pancreatic islets, *Diabetes* **39**, 519-522.

Hong, J.S. and Cooper-White, J.J., 2007, Drop formation of a

non-Newtonian fluid in a flow-focusing microfluidic channel, in preparation.

Jeong, W.J., J.Y. Kim, S.J. Kim, S.H. Lee, G. Mensing, and D.J. Beebe, 2004, *Lab Chip* **4**, 576-580.

Jeong, W.J., J.Y. Kim, J. Choo, E.K. Lee, C.S. Han, D.J. Beebe, G.H. Seong and S.H. Lee, 2005, *Langmuir* **21**, 3738-3741.

Khattak, S.F., S.R. Bhatia and S.C. Roberts, 2005, Pluronic F127 as a cell encapsulation material: utilization of membrane-stabilizing agents, *Tissue Engineering* **11(5/6)**, 974-983.

Lacy, P.E. and M. Kostianovsky, 1967, Method for the isolation of intact islets of Langerhans from the rat pancreas. *Diabetes* **16**, 35-39.

Li, C.H., 2006, *Microfluidic Lab-on a-chip for chemical and biological analysis and discovery*, CRC press.

Lim, F. and A.M. Sun, 1980, Microencapsulated islets as bioartificial endocrine pancreas, *Science* **210**, 908-910.

Microprobes, Product information MP07013, LIVE/DEAD Reduced Biohazard Viability/Cytotoxicity Kit#1 (L-7013).

Microprobes, Product information MP03224, LIVE/DEAD Viability/Cytotoxicity Kit for mammalian cells.

Rayleigh, L., 1879, On the capillary phenomena of jets, *Proc. R. Soc.* **29**, 71-97.

Strand, B.L., 2001, Poly-L-lysine induces fibrosis on alginate microcapsules via the induction of cytokines, *Cell Transplant.* **10**, 263-275.

Sun, Y.L., X.J. Ma, D.B. Zhou, I. Vacek and A.M. Sun, 1996, Normalization of diabetes in spontaneously diabetic cynomologous monkeys by xenografts of microencapsulated porcine islets without immunosuppression, *J. Clin. Invest.* **98**, 1417-1422.

Sugiura, S., T. Oda, Y. Izumida, Y. Aoyagi, M. Satake, A. Ochiai, N. Ohkohchi and M. Nakajima, 2005, Size control of calcium alginate beads containing living cells using micro-nozzle array, *Biomaterials* **26**, 3327-3331.

Utada, A.S., E. Lorenceau, D.R. Link, P.D. Kaplan, H.A. Stone and D.A. Weitz, 2005, Monodisperse double emulsions generated from a microcapillary device, *Science* **308**, 537-541.

Xu, Q., M. Nakajima, 2004, The generation of highly monodisperse droplets through the breakup of hydrodynamically focused microthread in a microfluidic device, *App. Phy. Lett.* **85(17)**, 3726-3728.